

Probing quantum features of photosynthetic organisms

Tanjung Krisnanda,¹ Chiara Marletto,² Vlatko Vedral,^{2,3} Mauro Paternostro,⁴ and Tomasz Paterek^{1,5}

¹*School of Physical and Mathematical Sciences, Nanyang Technological University, 637371 Singapore, Singapore*

²*Clarendon Laboratory, University of Oxford, Parks Road, Oxford OX1 3PU, United Kingdom*

³*Centre for Quantum Technologies, National University of Singapore, 117543 Singapore, Singapore*

⁴*School of Mathematics and Physics, Queen's University, Belfast BT7 1NN, United Kingdom*

⁵*MajuLab, CNRS-UNS-NUS-NTU International Joint Research Unit, UMI 3654 Singapore, Singapore*

Recent experiments have demonstrated strong coupling between living bacteria and light. Here we propose a scheme to infer quantumness of the light-bacteria correlations, as characterised by the presence of quantum discord, without requiring any knowledge of their mutual interactions, and by measuring only the light's degrees of freedom. This is achieved by monitoring the dynamics of the entanglement between few optical modes (probes) that interact independently with the bacteria. When the (light-sensitive part of) bacterium is modelled as a collection of two-level atoms we find that the steady state entanglement between the probes is independent of the initial conditions, is accompanied by entanglement between probes and bacteria, and provides independent evidence of the strong coupling between them.

There is no a priori limit on the complexity, size or mass of objects to which quantum theory is applicable. Yet, whether or not the physical configuration of macroscopic systems could showcase quantum coherences has been the subject of a long-standing debate. The pioneers of quantum theory, such as Schrödinger [1] and Bohr [2], wondered about whether there might be limitations to living systems obeying the laws of quantum theory. Wigner even claimed that their behaviour violates unitarity [3].

A striking way to counter such claims on the implausibility of macroscopic quantum coherence would be the successful preparation of quantum superposition states of living objects. A direct route towards such goal is provided by matter-wave interferometers, which have already been instrumental in observing quantum interference from complex molecules [4], and are believed to hold the potential to successfully show similar results for objects as large as viruses in the near future.

However, other possibilities exist that do not make use of interferometric approaches. An instance of such alternatives is to interact a living object with a quantum system in order to generate quantum correlations. Should such correlations be as strong as entanglement, measuring the quantum system in a suitable basis could project the living object into a quantum superposition. However, requesting the establishment of entanglement is, in general, not necessary as the presence of quantum discord, that is a weaker form of quantum correlations, would already provide evidence that the Hilbert space spanned by the living object must contain quantum superposition states [5–9]. For example, by operating on the quantum system alone one could remotely prepare quantum coherence in the living object [10].

A promising step in this direction, demonstrating strong coupling between living bacteria and optical fields and suggesting the existence of entanglement between them [11], has recently been realised [12]. However, the experimental results reported in Ref. [12] can as well be explained by a fully classical model [11, 13], which calls

loud for the design of a configuration with more conclusive interpretations.

In this paper we make a proposal in such a direction by designing a thought experiment that does not require any direct operation on the bacteria nor does it rely on any knowledge about their interaction with light. We then propose a plausible model of such interactions and demonstrate within this model that steady-state entanglement between the modes of the optical probes is always accompanied by light-bacteria entanglement, which is in turn empowered by the strong coupling between such systems. Our proposal thus delineates a path towards the inference of non-classicality of living organisms through their ability to establish quantum correlations with easily accessed probing systems.

The thought experiment and its model. Consider the setup presented in Fig. 1. The bacteria are inside a driven single-sided multimode Fabry-Perot cavity where they interact independently with a few cavity modes. It is crucial for the method that these modes do not interact

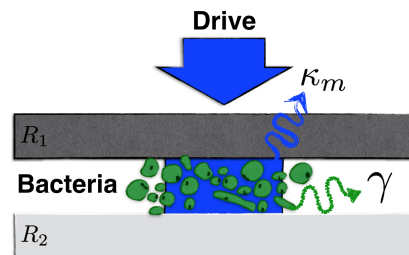


FIG. 1. We consider a driven single-sided multimode Fabry-Perot cavity embedding green sulphur bacteria. Here, R_1 is the input mirror, while R_2 is a perfectly reflecting end mirror. A few cavity modes individually interact with the bacteria, but not with each other. Both bacteria and cavity modes are open systems. In particular, the interaction between bacteria and their environment results in the energy decay rate 2γ . The m^{th} cavity field mode experiences energy dissipation at a rate $2\kappa_m$.

directly, but only via the bacteria. This can be realised in practice by choosing cavity modes that are orthogonally polarised or sufficiently distant in frequency. Both bacteria and cavity are treated as open systems, each coupled to its own local environment.

Under such general conditions, if one starts from a global product state of the system, intermodal entanglement cannot be established if, at all times, there is no quantum discord between cavity modes and bacteria [14]. Conversely, any observed intermodal entanglement witnesses the presence of quantum discord. We stress that, for such a revelation of non-classicality of the bacteria, their state does not have to be measured and their interaction with the optical modes can remain unspecified. This embodies the methodological pillar of our proposal for the probing of quantum features in living organisms.

In order to make such proposal more concrete, we now study a specific model for the energy of the bacteria and their interactions with light in order to demonstrate that there is observable intermodal entanglement. We consider a photosynthetic bacterium, *Chlorobaculum tepidum*, that is able to survive in extreme environments with almost no light [15]. Each bacterium, which is approximately $2\mu\text{m} \times 500\text{nm}$ in size, contains 200 chlorosomes, each having 200,000 bacteriochlorophyll *c* (BChl *c*) molecules. Such pigment molecules serve as excitons that can be coupled to light [12, 16].

Following the proposal in Ref. [11], we model the pigment molecules of the bacteria as a collection of N two-level atoms. For simplicity, we assume that all of them have the same frequency ω_b and are coupled through a dipole-like mechanism to each light mode. This simple model was already shown to be capable of explaining the results of recent experiments [12]. For $N \gg 1$, such collection of two-level systems can be approximated to a spin $N/2$ angular momentum. In the low-excitation approximation (which we will justify later), such angular momentum can be mapped into an effective harmonic oscillator through the use of the well-known Holstein-Primakoff transformation [17]. This allows us to cast the energy of the overall system as

$$H = \sum_m \hbar\omega_m \hat{a}_m^\dagger \hat{a}_m + \hbar\omega_b \hat{b}^\dagger \hat{b} + \sum_m \hbar G_m (\hat{a}_m + \hat{a}_m^\dagger) (\hat{b} + \hat{b}^\dagger) + \sum_m i\hbar E_m (\hat{a}_m^\dagger e^{-i\Omega_m t} - \hat{a}_m e^{i\Omega_m t}). \quad (1)$$

Here, $m = 1, \dots, M$ is the label for the m^{th} cavity mode, whose annihilation (creation) operator is denoted as \hat{a}_m (\hat{a}_m^\dagger) and having frequency ω_m . Moreover, \hat{b} and \hat{b}^\dagger denote the bosonic annihilation and creation operators for the harmonic oscillator describing the bacteria, which is coupled to the m^{th} cavity field at rate G_m . The collective form of the coupling allows us to write $G_m = g_m \sqrt{N}$ with $g_m = (\vec{\mu} \cdot \hat{E}) \sqrt{\pi \hbar c / n_r^2 \lambda_m \varepsilon_0 V_m}$, where $\vec{\mu}$ is the dipole moment of the two-level transition, \hat{E} a unit vector in the direction of cavity electric field, n_r refractive index of medium, and λ_m wavelength of the m^{th} cavity mode

with volume V_m [18]. The cavity is driven by a multi-mode laser, each mode having frequency Ω_m , amplitude $E_m = \sqrt{2P_m \kappa_m / \hbar \Omega_m}$, power P_m , and amplitude decay rate κ_m . It is important to notice that in Eq. (1) we have not invoked the rotating-wave approximation but actually retained the counter-rotating terms $\hat{a}_m \hat{b}$ and $\hat{a}_m^\dagger \hat{b}^\dagger$. These cannot be ignored in the regime of strong coupling and we will show that they actually play a crucial role in our proposal.

We assume the local environment of bacteria to give rise to Markovian open-system dynamics, which is modelled as decay of the two-level systems in their environment. On the other hand, the cavity modes are interacting with the electromagnetic environment outside the cavity, resulting in decay rate of each mode. We treat these environments as independent, i.e. they affect their open systems locally. In this case, the dynamics of optical modes and bacteria can be written using the standard Langevin formulation in Heisenberg picture. This gives the following equations of motion, taking into account noise and damping terms coming from interactions with the local environments

$$\begin{aligned} \dot{\hat{a}}_m &= -(\kappa_m + i\omega_m) \hat{a}_m - iG_m (\hat{b} + \hat{b}^\dagger) + E_m e^{-i\Omega_m t} \\ &\quad + \sqrt{2\kappa_m} \hat{F}_m, \\ \dot{\hat{b}} &= -(\gamma + i\omega_b) \hat{b} - i \sum_m G_m (\hat{a}_m + \hat{a}_m^\dagger) + \sqrt{2\gamma} \hat{F}_b, \end{aligned} \quad (2)$$

where γ is the amplitude decay rate of the bacterial system. \hat{F}_m and \hat{F}_b are operators describing independent zero-mean Gaussian noise affecting the m^{th} cavity field and bacteria respectively. The only correlation functions between these noises are $\langle \hat{F}_m(t) \hat{F}_m^\dagger(t') \rangle = \delta_{mm'} \delta(t - t')$ and $\langle \hat{F}_b(t) \hat{F}_b^\dagger(t') \rangle = \delta(t - t')$ [19, 20].

We express the Langevin equations in terms of mode quadratures. In particular, by using $\hat{x}_m \equiv (\hat{a}_m + \hat{a}_m^\dagger) / \sqrt{2}$ and $\hat{y}_m \equiv (\hat{a}_m - \hat{a}_m^\dagger) / i\sqrt{2}$ one gets a set of Langevin equations for the quadratures that can be written in a matrix equation $\dot{u}(t) = Ku(t) + l(t)$ with the vector $u = (\hat{x}_1, \hat{y}_1, \dots, \hat{x}_M, \hat{y}_M, \hat{x}_b, \hat{y}_b)^T$. Here, K is a square matrix with dimension $2(M + 1)$ describing the drift and l is a $2(M + 1)$ vector containing the noise and pumping terms (see Appendix A for explicit expressions). The solution to the Langevin equations is given by

$$u(t) = W_+(t)u(0) + W_+(t) \int_0^t dt' W_-(t') l(t'), \quad (3)$$

where $W_\pm(t) = \exp(\pm Kt)$.

As the Langevin equations are linear this dynamics preserves gaussian character of the initial state and hence our system is fully characterised by its covariance matrix. One can construct the covariance matrix as a function of time $V(t)$ from Eq. (3) (cf. Appendix B). Time evolution of important quantities can then be calculated from the covariance matrix, e.g. entanglement and excitation number (cf. Appendix C and D). We shall only be interested in the steady state, which is guaranteed when all

real parts of the eigenvalues of K are negative. In this case the covariance matrix satisfies Lyapunov-like equation

$$KV(\infty) + V(\infty)K^T + D = 0, \quad (4)$$

where $D = \text{Diag}[\kappa_1, \kappa_1, \dots, \kappa_M, \kappa_M, \gamma, \gamma]$. Note that the steady-state covariance matrix does not depend on the initial conditions, i.e. $V(0)$.

Let us suppose that initially $G_m = 0$, this can be done for example by choosing a cavity such that the optical modes supported and dipole moment of bacterial system are orthogonal or by filtering out polarisation in the direction of $\vec{\mu}$ (e.g. [21]). The cavity modes and bacteria can thus be assumed to be initially uncorrelated. In what follows, we start with vacuum state for the cavity modes and ground state for bacteria. The initial state of the bacteria is justified by the fact that $\hbar\omega_b \gg k_B T$, even at room temperature. The dynamics is then started by rotating the polarisation of cavity modes, i.e. turning on G_m .

Results. In order to maximise the free spectral range of the cavity, its size should be as small as possible. In the present case the bacteria themselves are about half a micron long. We therefore place the bacteria ($\omega_b = 2.5 \times 10^{15}$ Hz) in a single-sided Fabry-Perot cavity of length $L = 567$ nm (cf. Fig. 1) [12]. The refractive index due to aqueous bacterial solution embedded in the cavity is $n_r \approx 1.33$, which implies the frequency of the m^{th} cavity mode $\omega_m = m\pi c/n_r L \approx 1.25m \times 10^{15}$ Hz. The mirrors are engineered such that $R_2 = 100\%$ and $R_1 = 5\%$. We assume the reflectivities are the same for all the optical modes giving $\kappa_m \approx 3 \times 10^{14}$ Hz. The decay rate of the excitons can be approximated as $\gamma = 1/2\tau_b$ where $\tau_b = 2\hbar/\Gamma_b$ is the coherence time with Γ_b the FWHM linewidth [22]. The FWHM linewidth is taken to be 130 meV [12], giving $\gamma \approx 7.8 \times 10^{12}$ Hz. We take all the spectral components of the driving laser to have the same power $P_m = 50$ mW and frequency $\Omega_m = \omega_m$. By using the mode volume $V_m = 2\pi L^3/m(1 - R_1)$ [23], we can express the interaction strength as $G_m = m\tilde{G}$, where we define $\tilde{G} \equiv (\vec{\mu} \cdot \vec{E})\sqrt{\hbar c(1 - R_1)N/4n_r^3\epsilon_0 L^4}$. This quantity is a rate that characterises the base collective light-bacteria interaction strength. Instead of fixing the value of \tilde{G} , we vary this quantity $\tilde{G} = [0, 0.1]\omega_b$, which is within experimentally achievable regime (cf. Refs. [11, 12]).

Entanglement dynamics (logarithmic negativity) is illustrated in Fig. 2, where we show the existence of steady-state entanglement between the cavity modes. Fig. 2 (a) shows that contribution to 12 : 34 entanglement from the 5th and 6th mode is not significant. Therefore, we consider 4 cavity modes in all other calculations. Apart from bipartition 12 : 34 one can also use other bipartitions as indication of non-classical bacteria, exemplary ones are presented in Fig. 2 (b). In recent experiments, the rate \tilde{G} was shown to be $0.03\omega_b$ [12]. In our calculations we vary this rate, e.g. see Fig. 2 (c) and (d). It is also apparent that entanglement between cavity

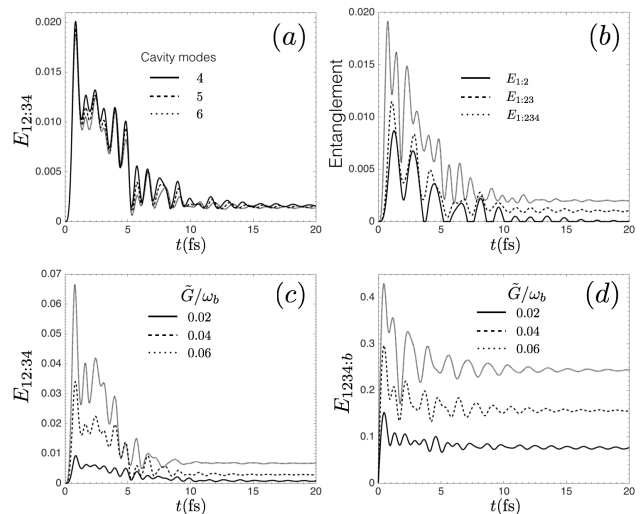


FIG. 2. Dynamics of entanglement (logarithmic negativity). (a) Bipartite entanglement between cavity modes 1, 2 and 3, 4 taking into account up to 4, 5, and 6 cavity modes, showing that higher modes do not contribute to steady state entanglement. (b) Exemplary entanglement between cavity modes in different bipartitions. (c) Entanglement in the partition 12 : 34 with varying base interaction rate. (d) Entanglement between cavity modes and bacteria with varying base interaction strength. The rate for (a) and (b) is $\tilde{G} = 0.03\omega_b$ [12]. We consider four cavity modes in (b), (c), and (d). In all considered cases, steady state entanglement is reached in ~ 20 fs.

modes and bacteria $E_{1234:b}$ grows much faster than entanglement between cavity modes. More precisely, nonzero $E_{12:34}$ implies nonzero $E_{1234:b}$. Moreover, it can be seen that it takes ~ 20 fs to reach the steady-state regime, which is much faster than relaxation processes (\sim ps) occurring within green sulphur bacteria [16].

In the steady state regime, we calculated the entanglement in the partition 12 : 34 and 1234 : b, cf. Fig. 3. One can see that the bacteria can be strongly correlated with cavity modes, much stronger than entanglement between the modes. The latter is in the order of $10^{-2} - 10^{-3}$.

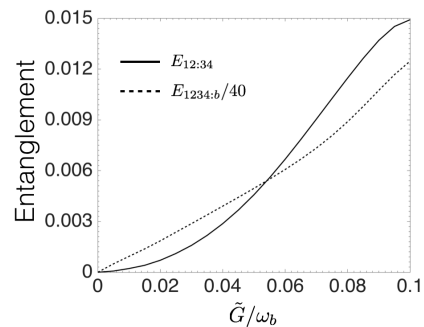


FIG. 3. Steady-state entanglement between cavity modes 12 : 34 and cavity modes-bacteria 1234 : b with varying base coupling strength $\tilde{G} = [0, 0.1]\omega_b$. Note that entanglement with bacteria is rescaled by a factor of 40.

We note that entanglement in the range 10^{-2} has already been observed experimentally between mechanical motion and microwave cavity fields [24].

In order to justify the low atomic excitation limit we plot the evolution of excitation of bacteria (together with the number of photons in different cavity modes) in Fig. 4. It shows that excitation numbers are oscillating in the “steady state”. They are caused by interactions between light and bacteria (Rabi-like oscillations). Setting the interactions off ($G_m = 0$) produces constant steady-state values (dashed lines in Fig. 4) given by $E_m^2/(\kappa_m^2 + \Delta_m^2) \propto P_m$, where $\Delta_m = \Omega_m - \omega_m$ is the laser-cavity detuning. Note that photon number of the 2nd cavity mode (solid cyan line) is showing oscillations well below its “off-interaction” value (dashed cyan line). This is because ω_2 is in resonance with the frequency of the atomic transition ω_b . Finally, we note that the excitation number of the bacterial system can reach ~ 3000 , and with $\sim 10^8$ actively coupled dipoles in the cavity [12] it gives $\sim 3 \times 10^{-3}\%$ excitation, which justifies the low-excitation approximation.

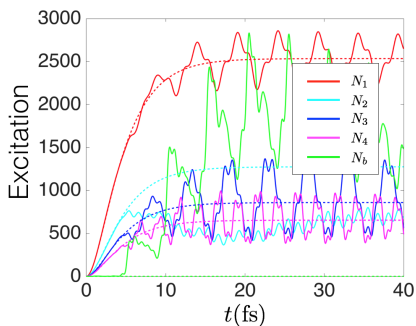


FIG. 4. Evolution of photon number of cavity modes N_1 , N_2 , N_3 , N_4 and excitation of bacteria N_b for coupling strength $\tilde{G} = 0.03 \omega_b$ [12] (solid lines). Dashed lines represent the evolution when the interactions between bacteria and light are absent ($\tilde{G}_m = 0$).

Discussion. It should be pointed out that covariance matrix $V(t)$ (and hence the entanglement) does not depend on the power of the lasers. This is a consequence of the dipole-dipole coupling and classical treatment of the driving field (see Appendix B). Hence, the system gets entangled also in the absence of the lasers. There is no fundamental reason why this entanglement with vacuum could not be measured, but practically it is preferable to pump the cavity in order to improve the signal-to-noise ratio. Of course quantities other than entanglement may depend on driving power, for example the light intensity inside the cavity as shown in Fig. 4.

This finding is quite different from results in optomechanical system where the covariance matrix depends on laser power [14, 25]. The origin of this discrepancy is the nature of the coupling. For example, in optomechanical system consisting of a single cavity mode \hat{a} and a mechanical mirror \hat{b} the coupling is proportional to $\hat{a}^\dagger \hat{a} \hat{x}_b$, which is third order in operators [26]. This results in effective

coupling strength being proportional to the classical cavity signal α after linearisation of the Langevin equations. This classical signal enters the covariance matrix via effective coupling strength and introduces the dependence on driving power.

We also performed similar calculations in which we neglected the counter rotating terms in Eq. (1), the model known as Tavis-Cummings. This resulted in no entanglement generated in the steady state and can be intuitively understood as follows. Since the steady-state covariance matrix does not depend on initial state, we might start with all atoms in the ground state and vacuum for the light modes. It can be argued in Schrödinger picture that this will be the state of affairs at any time as we only consider energy preserving terms in the light-bacteria coupling. Therefore, nonzero entanglement observed in experiments will provide evidence of the counter rotating terms in the coupling.

Conclusions. We have proposed a setup for the inference of non-classicality of photosynthetic organisms. Our scheme is based on coupling the organisms to a few optical modes in a driven cavity. Our detection method does not require detailed modelling of the organisms and makes no assumptions about interaction between them and the probes. It only requires that the organisms independently interact with each probe for some time after which one estimates entanglement between the probes. Non-classicality is inferred by the observation of nonzero entanglement. We have performed simulations of this system within a plausible model using recent experimental parameters. Calculations confirm measurable steady-state entanglement which implies entanglement with the organisms and provides evidence for strong coupling.

Acknowledgments. This work is supported by the National Research Foundation (Singapore) and Singapore Ministry of Education Academic Research Fund Tier 2 Project No. MOE2015-T2-2-034. CM is supported by the Templeton World Charity Foundation and the Eutopia Foundation. MP is supported by the SFI-DfE Investigator Programme (Grant 15/IA/2864) and a Royal Society Newton Mobility Grant (NI160057).

Appendix A: Evolution of quadratures

The Langevin equations for the quadratures can be written in a simple matrix equation $\dot{u}(t) = Ku(t) + l(t)$, with the vector $u = (\hat{x}_1, \hat{y}_1, \dots, \hat{x}_M, \hat{y}_M, \hat{x}_b, \hat{y}_b)^T$ and

$$K = \begin{pmatrix} I_1 & \mathbf{0} & \cdots & \mathbf{0} & L_1 \\ \mathbf{0} & I_2 & \cdots & \mathbf{0} & L_2 \\ \vdots & \vdots & \ddots & \vdots & \vdots \\ \mathbf{0} & \mathbf{0} & \cdots & I_M & L_M \\ L_1 & L_2 & \cdots & L_M & I_b \end{pmatrix}, \quad (\text{A1})$$

where the components are 2×2 matrices given by

$$I_m = \begin{pmatrix} -\kappa_m & \omega_m \\ \omega_m & -\kappa_m \end{pmatrix}, \quad L_m = \begin{pmatrix} 0 & 0 \\ -2G_m & 0 \end{pmatrix},$$

$$I_b = \begin{pmatrix} -\gamma & \omega_b \\ -\omega_b & -\gamma \end{pmatrix}, \quad (\text{A2})$$

and $\mathbf{0}$ is a 2×2 zero matrix. We split the last term into two parts, representing the noise and pumping respectively, i.e. $l(t) = n(t) + p(t)$ where

$$\frac{n(t)}{\sqrt{2}} = \begin{pmatrix} \sqrt{\kappa_1} \hat{X}_1(t) \\ \sqrt{\kappa_1} \hat{Y}_1(t) \\ \vdots \\ \sqrt{\kappa_M} \hat{X}_M(t) \\ \sqrt{\kappa_M} \hat{Y}_M(t) \\ \sqrt{\gamma} \hat{X}_b(t) \\ \sqrt{\gamma} \hat{Y}_b(t) \end{pmatrix}, \quad \frac{p(t)}{\sqrt{2}} = \begin{pmatrix} E_1 \cos \Omega_1 t \\ -E_1 \sin \Omega_1 t \\ \vdots \\ E_M \cos \Omega_M t \\ -E_M \sin \Omega_M t \\ 0 \\ 0 \end{pmatrix}. \quad (\text{A3})$$

We have also used quadratures for the noise terms, i.e. through $\hat{F}_m = (\hat{X}_m + i\hat{Y}_m)/\sqrt{2}$.

The solution to the Langevin equations is given by Eq. (3) in the main text. This allows numerical calculation for expectation value of the quadratures as a function of time, i.e. $\langle u_i(t) \rangle$ is given by the i^{th} element of

$$W_+(t)\langle u(0) \rangle + W_+(t) \int_0^t dt' W_-(t') p(t'). \quad (\text{A4})$$

Since every component of $p(t)$ is not an operator, we have $\langle p_k(t) \rangle = \text{tr}(p_k(t)\rho) = p_k(t)$. Also, we have used the fact that the noises have zero mean, i.e. $\langle n_k(t) \rangle = 0$.

Appendix B: Covariance matrix

Covariance matrix fully characterises our system and is defined as $V_{ij}(t) \equiv \langle \{\Delta u_i(t), \Delta u_j(t)\} \rangle / 2 = \langle u_i(t)u_j(t) + u_j(t)u_i(t) \rangle / 2 - \langle u_i(t) \rangle \langle u_j(t) \rangle$ where we have used $\Delta u_i(t) = u_i(t) - \langle u_i(t) \rangle$. This means that $p(t)$ does not contribute to $\Delta u_i(t)$ (and hence the covariance matrix) since $\langle p_k(t) \rangle = p_k(t)$. We can then construct the covariance matrix at time t from Eq. (3) without considering $p(t)$ as follows

$$\begin{aligned} V_{ij}(t) &= \langle u_i(t)u_j(t) + u_j(t)u_i(t) \rangle / 2 - \langle u_i(t) \rangle \langle u_j(t) \rangle \\ V(t) &= W_+(t)V(0)W_+^T(t) \\ &+ W_+(t) \int_0^t dt' W_-(t') D W_-^T(t') W_+^T(t), \end{aligned} \quad (\text{B1})$$

where $D = \text{Diag}[\kappa_1, \kappa_1, \dots, \kappa_M, \kappa_M, \gamma, \gamma]$ and we have assumed that the initial quadratures are not correlated with the noise quadratures such that the mean of the cross terms are zero. A more explicit solution of the covariance matrix, after integration in Eq. (B1), is given by

$$\begin{aligned} KV(t) + V(t)K^T &= -D + KW_+(t)V(0)W_+^T(t) \\ &+ W_+(t)V(0)W_+^T(t)K^T \\ &+ W_+(t)DW_+^T(t), \end{aligned} \quad (\text{B2})$$

which is linear and can be solved numerically.

The steady state is guaranteed when all real parts of the eigenvalues of K are negative, i.e. $W_+(\infty) = \mathbf{0}$. In this case the covariance matrix satisfies Eq. (4) from the main text.

Appendix C: Entanglement from covariance matrix

The covariance matrix V describing our system can be written in block form

$$V = \begin{pmatrix} L_{11} & L_{12} & \cdots & L_{1N} \\ L_{12}^T & L_{22} & \cdots & L_{2N} \\ \vdots & \vdots & \ddots & \vdots \\ L_{1N}^T & L_{2N}^T & \cdots & L_{NN} \end{pmatrix}, \quad (\text{C1})$$

where N is the total number of modes, which is $M + 1$ in our case. The block component L_{jk} is a 2×2 matrix describing local mode correlation when $j = k$ and intermodal correlation when $j \neq k$. An N -mode covariance matrix has symplectic eigenvalues $\{\nu_k\}_{k=1}^N$ that can be computed from the spectrum of matrix $|i\Omega_N V|$ [27] where

$$\Omega_N = \bigoplus_{k=1}^N \begin{pmatrix} 0 & 1 \\ -1 & 0 \end{pmatrix}. \quad (\text{C2})$$

For a physical covariance matrix $2\nu_k \geq 1$ [28].

Entanglement is calculated as follows. For example, the calculation in the partition 12 : 34 only requires the following covariance matrix

$$V_{1234} = \begin{pmatrix} L_{11} & L_{12} & L_{13} & L_{14} \\ L_{12}^T & L_{22} & L_{23} & L_{24} \\ L_{13}^T & L_{23}^T & L_{33} & L_{34} \\ L_{14}^T & L_{24}^T & L_{34}^T & L_{44} \end{pmatrix}, \quad (\text{C3})$$

that can be obtained from Eq. (C1). If the covariance matrix is not physical after partial transposition with respect to mode 3 and 4 (this is equivalent to flipping the sign of the operator \hat{y}_3 and \hat{y}_4 in V_{1234}) then our system is entangled. This unphysical V_{1234}^T is shown by its minimum symplectic eigenvalues $\tilde{\nu}_{\min} < 1/2$. Entanglement is then quantified by logarithmic negativity as follows $E_{12:34} = \max[0, -\ln(2\tilde{\nu}_{\min})]$ [29, 30]. Note that the separability condition, when $\tilde{\nu}_{\min} \geq 1/2$, is sufficient and necessary when one considers 1 : N mode partition [31], e.g. 1234 : b .

Appendix D: Excitation numbers

The excitation number of cavity modes and bacteria as a function of time can be calculated from $\langle u_i(t) \rangle$ and $V_{ii}(t)$. For example, the mean excitation number for the first cavity mode is given by

$$\langle N_1(t) \rangle = \langle \hat{a}_1^\dagger(t) \hat{a}_1(t) \rangle = \frac{1}{2} \left(\sum_{i=1}^2 (V_{ii}(t) + \langle u_i(t) \rangle^2) - 1 \right). \quad (\text{D1})$$

- [1] E. Schrödinger. *What is life?* (University Press: Cambridge, 1943).
- [2] N. Bohr. Light and Life. *Nature* **131**, 457 (1933).
- [3] E. Wigner. *The Probability of a Self-Reproducing Unit. Symmetries & Reflections* (Indiana University Press, Bloomington, 1967).
- [4] S. Gerlich, S. Eibenberger, M. Tomandl, S. Nimmrichter, K. Hornberger, P. J. Fagan, J. Tüxen, M. Mayor, and M. Arndt. Quantum interference of large organic molecules. *Nat. Commun.* **2**, 263 (2011).
- [5] L. Henderson and V. Vedral. Classical, quantum and total correlations. *J. Phys. A* **34**, 6899 (2001).
- [6] H. Ollivier and W. H. Zurek. Quantum discord: a measure of the quantumness of correlations. *Phys. Rev. Lett.* **88**, 017901 (2001).
- [7] L. C. Celeri, J. Maziero, and R. M. Serra. Theoretical and experimental aspects of quantum discord and related measures. *Int. J. Quant. Inf.* **9**, 1837 (2011).
- [8] K. Modi, A. Brodutch, H. Cable, T. Paterek, and V. Vedral. The classical-quantum boundary for correlations: discord and related measures. *Rev. Mod. Phys.* **84**, 1655 (2012).
- [9] G. Adesso, T. R. Bromley, and M. Cianciaruso. Measures and applications of quantum correlations. *J. Phys. A* **49**, 473001 (2016).
- [10] E. Chitambar, A. Streltsov, S. Rana, M. N. Bera, G. Adesso, and M. Lewenstein. Assisted distillation of quantum coherence. *Phys. Rev. Lett.* **116**, 070402 (2016).
- [11] C. Marletto, D. Coles, T. Farrow, and V. Vedral. Entanglement between living bacteria and quantized light witnessed by Rabi splitting. *arXiv preprint arXiv:1702.08075*, (2017).
- [12] D. Coles, L. Flatten, T. Sydney, E. Hounslow, S. Saikin, K. Semion, A. Aspuru-Guzik, V. Vedral, J. Tang, R. Taylor, J. Smith, and D. Lidzey. Polaritons in living systems: modifying energy landscapes in photosynthetic organisms using a photonic structure. *arXiv preprint arXiv:1702.01505*, (2017).
- [13] Y. Zhu, D. J. Gauthier, S. E. Morin, Q. Wu, H. J. Carmichael, and T. W. Mossberg. Vacuum Rabi splitting as a feature of linear-dispersion theory: Analysis and experimental observations. *Phys. Rev. Lett.* **64**, 21 (1990).
- [14] T. Krisnanda, M. Zuppardo, M. Paternostro, and T. Paterek. Revealing Nonclassicality of Inaccessible Objects. *Phys. Rev. Lett.* **119**, 120402 (2017).
- [15] R. E. Blankenship, J. M. Olson, and M. Miller. *Anoxygenic photosynthetic bacteria* (Springer, 1995).
- [16] D. Coles, Y. Yang, Y. Wang, R. T. Grant, R. A. Taylor, S. K. Saikin, A. Aspuru-Guzik, D. G. Lidzey, J. K. H. Tang, and J. M. Smith. Strong coupling between chlorosomes of photosynthetic bacteria and a confined optical cavity mode. *Nat. Commun.* **5**, 5561 (2014).
- [17] T. Holstein and H. Primakoff. Field dependence of the intrinsic domain magnetization of a ferromagnet. *Phys. Rev.* **58**, 1098 (1940).
- [18] M. Fox. *Quantum Optics-An Introduction* (Oxford Master Series, 2006).
- [19] C. W. Gardiner and P. Zoller. *Quantum noise* (Springer Science & Business Media, 2004).
- [20] D. F. Walls and G. J. Milburn. *Quantum optics* (Springer Science & Business Media, 2007).
- [21] J. Rosenberg, R. V. Shenoi, S. Krishna, and O. Painter. Design of plasmonic photonic crystal resonant cavities for polarization sensitive infrared photodetectors. *Opt. Express* **18**, 3672 (2010).
- [22] D. Bajoni. Polariton lasers. Hybrid light-matter lasers without inversion. *J. Phys. D: Appl. Phys.* **45**, 313001 (2012).
- [23] K. Ujihara. Spontaneous emission and the concept of effective area in a very short optical cavity with plane-parallel dielectric mirrors. *Jpn. J. Appl. Phys.* **30**, L901 (1991). Note that cavities with different geometries will have different mode volume formulae.
- [24] T. A. Palomaki, J. D. Teufel, R. W. Simmonds, and K. W. Lehnert. Entangling mechanical motion with microwave fields. *Science* **342**, 710 (2013).
- [25] M. Paternostro, D. Vitali, S. Gigan, M. S. Kim, C. Brukner, J. Eisert, and M. Aspelmeyer. Creating and probing multipartite macroscopic entanglement with light. *Phys. Rev. Lett.* **99**, 250401 (2007).
- [26] D. Vitali, S. Gigan, A. Ferreira, H. R. Böhm, P. Tombesi, A. Guerreiro, V. Vedral, A. Zeilinger, and M. Aspelmeyer. Optomechanical entanglement between a movable mirror and a cavity field. *Phys. Rev. Lett.* **98**, 030405 (2007).
- [27] C. Weedbrook, S. Pirandola, R. García-Patrón, N. J. Cerf, T. C. Ralph, J. H. Shapiro, and S. Lloyd. Gaussian quantum information. *Rev. Mod. Phys.* **84**, 621 (2012).
- [28] In ref. [27] the condition is $\nu_k \geq 1$. The absence of the factor of 2 is due to the setting of $\hbar = 2$.
- [29] G. Vidal and R. F. Werner. Computable measure of entanglement. *Phys. Rev. A* **65**, 032314 (2002).
- [30] G. Adesso, A. Serafini, and F. Illuminati. Extremal entanglement and mixedness in continuous variable systems. *Phys. Rev. A* **70**, 022318 (2004).
- [31] R. F. Werner and M. M. Wolf. Bound entangled gaussian states. *Phys. Rev. Lett.* **86**, 3658 (2001).